Int J Earth Sci (Geol Rundsch) (2003) 92:407–425
DOI 10.1007/s00531-003-0326-y

ORIGINAL PAPER

Achim Kopf · Annette Deyhle · Vasili Y. Lavrushin · Boris G. Polyak · Joris M. Gieskes · Guram I. Buachidze · Klaus Wallmann · Anton Eisenhauer

Isotopic evidence (He, B, C) for deep fluid and mud mobilization from mud volcanoes in the Caucasus continental collision zone

Received: 18 March 2002 / Accepted: 30 December 2002 / Published online: 18 June 2003

Abstract The Caucasian orogenic wedge formed as a consequence of the closure of the Tethyan Ocean, and numerous fields of active mud volcanoes pepper the area adjacent to the Black and Caspian Seas. Stable isotope ratios of boron, helium, and carbon have been measured for gas, fluid and sediment samples from active mud volcanoes of Taman Peninsula and Georgia to estimate the sources and mobilization depths of the fluid phase and mud. Boron concentrations in mud volcano fluids were found to be 5–35× higher than seawater. Fluid isotope ratios vary between δ^{11}B=22 and 39‰, while isotope ratios of the smectite- and illite-rich extruded mud are considerably depleted in heavy ^{11}B (δ^{11}B=–8 to +7‰). B contents of these muds are ~8× higher than modern marine sediments. This suggests that liquefaction prior to mud volcanism was accompanied by both B enrichment and isotope fractionation, most likely at an intermediate depth mud reservoir at 2–4 km.

The hydrocarbon-generating source beds to the mud volcanoes are located at 7 to >10 km depth in the folded Maikop Formation and are of proposed Oligocene–Miocene age. The most likely mechanism is re-hydration of these shales by both hydrocarbons and a geochemically mature fluid from greater depth within the orogenic wedge. Such a deep fluid source is supported by our results from gas analyses, which imply an admixture of minor amounts (less than 1%vol) of ^{3}He (Georgia), thermogenic ^{13}C in methane as well as "ultraheavy" ^{13}C in CO_2 (both Taman and Georgia). The overall results attest active local flow of geochemically different fluids along deep-seated faults penetrating the two study areas in the Caucasian orogenic wedge, with the waters as well as the gases coming from below the Maikop Formation.

Keywords Mud volcanism · Boron isotopes · Caucasus · Deep-seated fluids · Liquefaction

A. Kopf (✉) · A. Deyhle · J. M. Gieskes
SCRIPPS Institution of Oceanography, UCSD,
9500 Gilman Drive, La Jolla, CA, 92092-0220, USA
e-mail: akopf@ucsd.edu
Tel.: +1-858-8223362
Fax: +1-858-8223310

V. Y. Lavrushin · B. G. Polyak
Geological Institute,
Russian Academy of Science (GIN RAS),
Pyzhevskii per.7, 109107 Moscow, Russia

G. I. Buachidze
Institute of Hydrogeology and Engineering Geology,
Georgian Academy of Science,
prosp. Rustaveli 31, 380008 Tbilisi, Georgia

K. Wallmann · A. Eisenhauer
GEOMAR Research Centre,
Wischhofstrasse 1–3, 24148 Kiel, Germany

Introduction

Mud volcanism and diapirism are global phenomena both onshore and offshore, and have previously been related to buried thick argillaceous sediment and petroleum reservoirs (e.g., Higgins and Saunders 1974; Kopf 2002). Extrusion of fluid-laden muds has been demonstrated to be an efficient mechanism of dewatering collisional environments (like accretionary prisms; e.g., Brown and Westbrook 1988; Kopf et al. 2001). Main driving forces are under-compaction of sediment and pore fluid overpressures and/or the formation and migration of hydrocarbon gas (e.g., Brown 1990). Most of this gas has been demonstrated to be methane, with less than 5% of H_2S, CO_2, or higher hydrocarbons (e.g., Limonov et al. 1995).

In the Caucasus, mud volcanism is known in various regions, e.g., the Kerch, Taman- and Crimea Peninsulas, the Kura region of Georgia, and many areas of Azerbaijan (e.g., Jakubov et al. 1971; Valyaev et al. 1985; Lavrushin et al. 1996). This must be viewed as a consequence of marine, smectite-rich sediments, which underwent burial due to incorporation into orogenesis after closure of the Tethys ocean. Recent industry 3D seismic data indicate that mud ascent takes place along narrow, deep-seated fault zones (Cooper 2001).

In this study, we use boron, helium and carbon stable isotopes:

1. to characterize B enrichment vs. depletion and $\delta^{11}B$ isotopes in mud volcano sediments and fluids as a tracer for increasing burial, deep fluid-rock interaction, and clues to mud mobilization and extrusion dynamics;
2. to use $\delta^{13}C$ signatures from CO_2 and hydrocarbon gas as indicators for elevated temperatures (i.e., deep burial);
3. to elucidate a contribution of crustal (and possibly mantle) He to the fluid phase and, hence, to extrusion dynamics as well as geochemical recycling;
4. to test whether the prominent continuous mud volcanic activity in the Caucasus is a function of the tectonic movements that release overpressured mud at depth, or whether re-hydration (i.e., liquefaction) of already consolidated mudstone feeds mud volcanism;
5. to identify possible repercussions of sediment liquefaction, mobilization and extrusion on readsorption and geochemical cycling of boron (and other mobile elements).

Previous mud volcano studies

Mud volcanism is a world-wide phenomenon, both on the seafloor and on land (see reviews by Higgins and Saunders 1974; Kopf 2002). Since its discovery on Java in the early 19th century (Goad 1816), it has been described by numerous workers (e.g., Abich 1863), but until recent improvements of marine geophysical data acquisition its significance has not been fully acknowledged. As a result of the tremendous efforts and submarine drilling and sampling during the last few decades, however, some light has been shed on the mechanism of mud extrusion as well as the source of the components involved (e.g., Brown 1990; Robertson et al. 1996; Kopf et al. 2001).

Mud volcanoes (MVs) occur in collisional (e.g., Brown and Westbrook 1988; Yassir 1989; Brown 1990) and transtensional settings (e.g., Limonov et al. 1995) on the seafloor, as well as on land (e.g., Higgins and Saunders 1974). The features are usually short-lived structures (<1 Ma), and vary considerably in both size and shape. Mud volcanoes contribute considerably to emission of greenhouse gases, namely CH_4 (e.g., Jakubov et al. 1971; Lavrushin et al. 1996), and also play an important role in fluid transfer from the sediment/lithosphere to the hydrosphere/atmosphere (Kopf et al. 2001). Irrespective of the different scenarios in which mud volcanoes occur, the driving force of ascent and extrusion is negative buoyancy. In general, a less dense, often fluid- and gas-rich, argillaceous reservoir at depth is overlain by compacted or cemented rock. As a consequence, excess pore fluid overpressures may evolve and cause either diapirism or diatremes (Brown 1990). The behavior and extrusion dynamics of such undercompacted mud has been subject to various hypotheses (see Kopf 2002), especially since the surface edifice does not always allow a detailed interpretation of the subsurface structure.

Mud extrusion in the Caucasus area is abundant in a variety of countries such as Georgia, Azerbaijan and Turkmenistan (Fig. 1), as has been detailed by Lavrushin et al. (1996). Its general significance as an important dewatering and de-volatilization mechanism during orogenesis is illustrated by the large size of the features as well as frequent eruptions during historic time (e.g., Jakubov et al. 1971; Cooper 2001).

Tectonic setting and regional geology of the Caucasus region

The present-day Caucasus region is dominated by thrust faulting due to continental collision (Mattauer 1968), having also caused prominent vertical movements and major strike-slip faulting in preferably NNE- and NNW-striking directions (Zonenshain and Le Pichon 1986). The geological history is complex, and is summarized here only very briefly (for details, see Dercourt et al. 1986). During Jurassic to Paleogenic time, subduction of Tethyan seafloor occurred along the southern margin of the Turkish and Iranian blocks, with calc-alkaline arc volcanism and a wide backarc basin system. During the early Miocene, Red Sea spreading was initiated, and the Arabian plate migrated northward, accompanied by a reduction in width of the Tethys. After its closure (~20 Ma), subduction shifted to the north. As a result of the indentation of the Arabian block, the continuous backarc basin was separated, and oceanic crust remained only in the Black Sea and southern Caspian Sea (Philip et al. 1989). The continuous northward drift of the Anatolian Plate led to initial continental collision expressed by the formation of the Lesser Caucasus, and the subsequent surrection of the Great Caucasus during Middle Pliocene (Fig. 1). At present, continental convergence continues with a rate of ~30 mm/a east and 10 mm/a west of the intersecting strike slip fault (Fig. 1). Most of the modern tectonic activity is localized along these faults (Philip et al. 1989).

A simplified tectonic map (Fig. 1) shows the main units surrounding the Great Caucasus from north to south:

- the Russian platform.
- the Kuban Basin (including the Crimea and Taman Peninsulas) and Terek-Caspian foredeeps separating the epi-Hercinian Scythian Plate from the Alpine mega-anticlinorium of the Greater Caucasus (including the Dagestan wedge in its north-eastern segment).
- the Rioni Basin (opening into the Black Sea) and Kura foredeep (extending into the Caspian Sea), both intermountaine basins.
- the Lesser Caucasus mega-anticlinorium and Talesh block in Georgia.

Hence, the two areas of this study are located in tectonically distinct regions. In the east, the Georgia mud

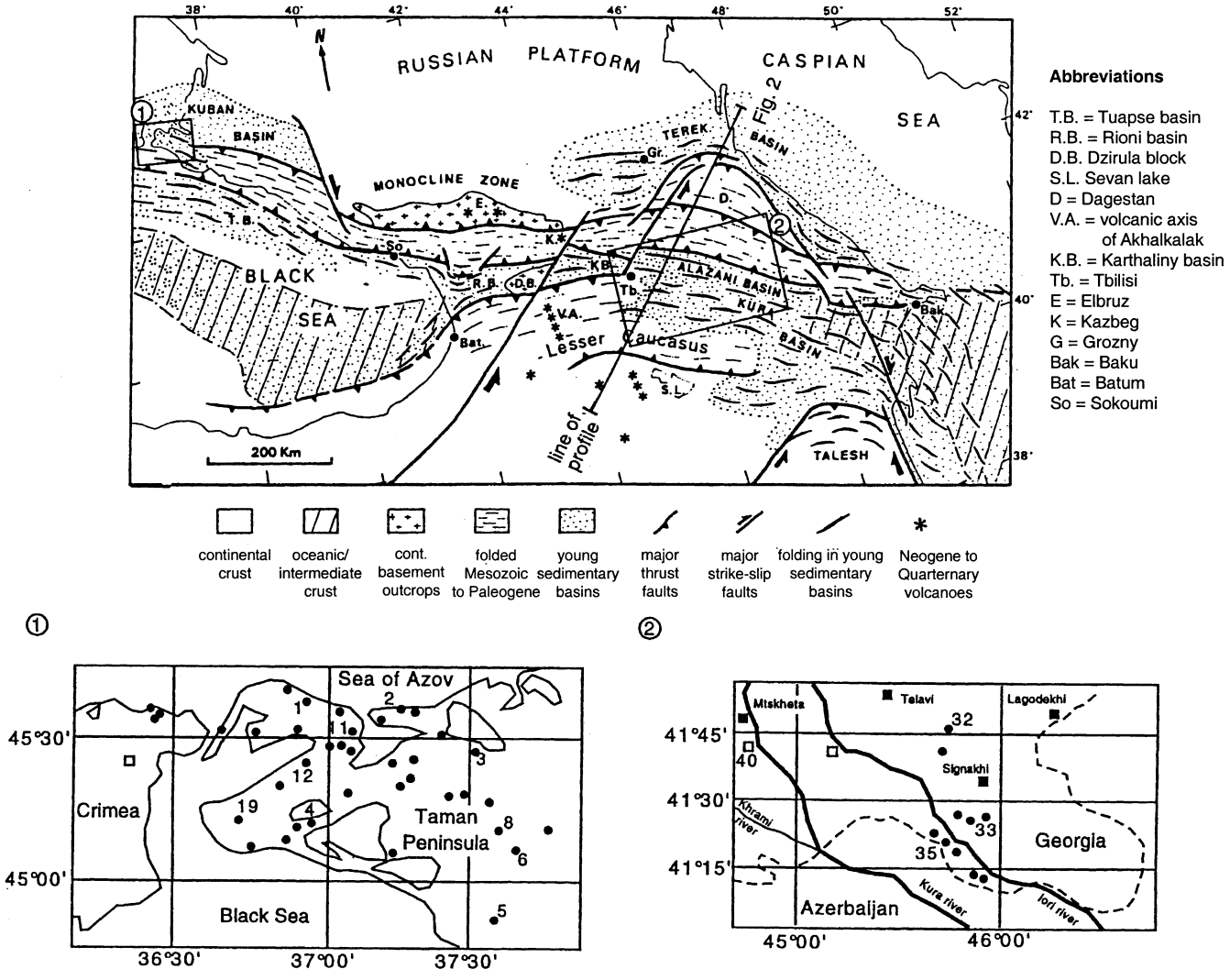

Fig. 1 Outline map of the Great Caucasus region, with *insets* showing the location of the mud extrusion domains in the east (*1* Taman Peninsula) and the west (*2* Georgia). The location of the cross section in Fig. 2 is illustrated by an *end-marked line*. In the detailed maps *1* and *2*, *dots* represent mud volcanoes; *numbers* of these mud volcanoes refer to Table 4, second column from left. *Open squares* are oil company boreholes; *solid squares* are towns. Modified from Philip et al., (1989) and Lavrushin et al. (1996)

volcanoes (MVs) occur in the Lesser Caucasus in a zone where the Arabian block is indenting (Fig. 1, inset 2). Here, Meso- and Cenozoic sediments of the Dagestan block (Fig. 1) are thrust beneath the northern hinterland. It is bordered to the south by Jurassic to Cretaceous folded and faulted rocks of the Great Caucasus axial zone, which itself is thrusting to the south over the Kura Basin (Figs. 1, 2). The latter consists of a very thick sequence of Paleogene to Quaternary marine sediments, which show imbricate stacking. These deposits are interpreted as an accretionary prism, having accumulated material from the latest Tethyan seafloor (as illustrated schematically in Fig. 2A; see also summary in Robertson 1998). The Georgian mud volcanoes occur in the frontal part of the continental collision zone (Fig. 2, SW part of profile), and originate from the ancient accretionary prism of the Kura Basin. By comparison, the Taman MVs are situated further northwest in the Great Caucasus (Fig. 1, inset 1). Between the northern border of the Black Sea (a remainder of the Tethyan backarc basin system) and the axial zone of the Great Caucasus, a sedimentary fill of Neogene to Quaternary age has accumulated. Tectonic shortening is more intense in the main orogenic collision zone, and faulting roots much deeper (see Fig. 2B).

Mud volcanoes are abundant in Georgia as well as Taman (e.g., Jakubov et al. 1971), and are largely of cone-shaped, flat-topped geometry (Fig. 3). The features reach several hundreds of meters (to more than 2 km) in diameter, and are usually several tens to hundreds of meters high (e.g., Tamrazyan 1972). Maximum sizes are up to 600 m height and 10 km^2 in area (Jakubov et al. 1971). Mud and fluids extrude as small cones, but may also form mud pools in the crestal region of the MV (Fig. 3B, C). Eruptions are accompanied by expulsion of mud breccias (i.e., clay-rich mud with rock fragments of the overlying successions), water, and gas, the latter of

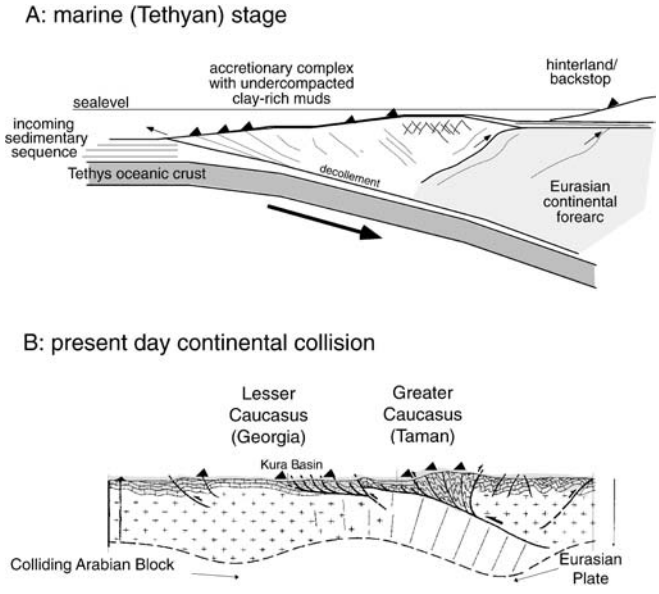

Fig. 2 **A** Schematic cross section of accretion and mud volcanism (*black triangles*) during the marine stage prior to closure of the Tethyan ocean; **B** geological cross section across the Lesser and Greater Caucasus, showing the present-day stage of continental collision with abundant mud volcanism. All oceanic crust has been subducted. For location of the cross section see Fig. 1 Note that mud volcanoes are not to scale! Modified from Philip et al. (1989)

which frequently self-ignites (e.g., Bagirov et al. 1996). For the entire Caucasus region, the Oligocene-Miocene Maikop Formation, a sedimentary succession of rapidly deposited, thick clastic rocks, has been suggested to be the source layer for mud volcanism (e.g., Lavrushin et al. 1996). As a function of complex folding and faulting, the Maikop shales occur at depths of 4 to more than 10 km, but in places show a second, intermediate depth mud reservoir in ~2 km (Cooper 2001).

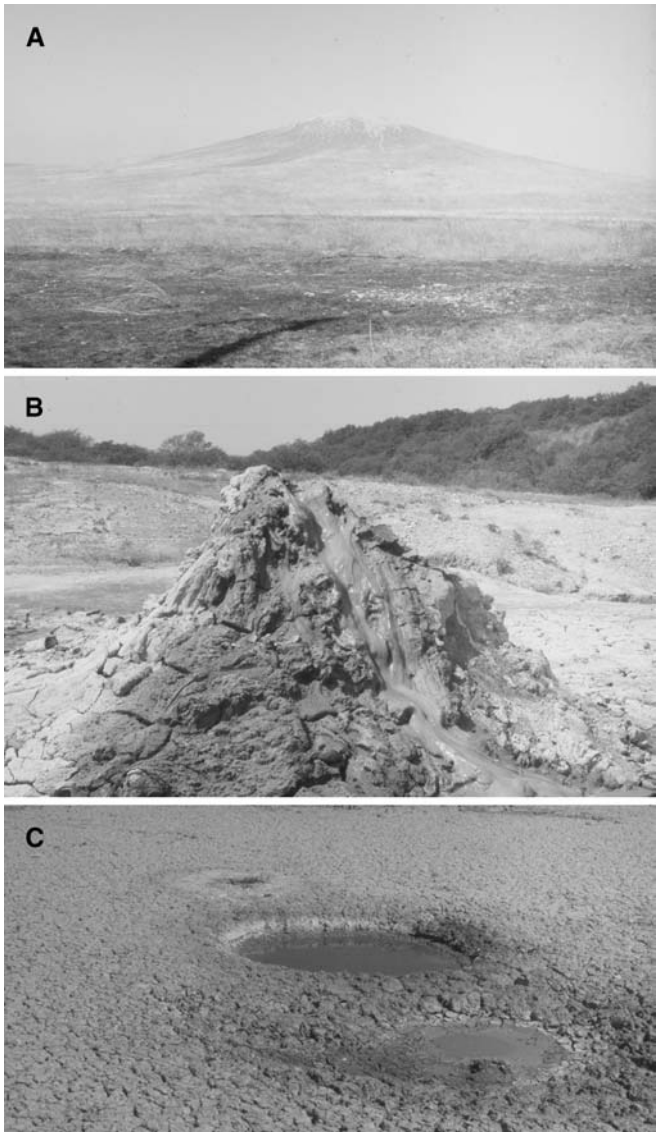

Fig. 3 **A** Photograph of Ahtanizovsky mud volcano; **B** small cone of recently extruded mud on Shugo mud volcano; **C** mud pools on the partly dried crestal plateau of Shapurski mud volcano

Sampling and experimental methods

Sampling

Free gas bubbles emanating from the aqueous phase at the MV craters were collected by placing mud volcano pore water in 220 cm^3 glass containers; after almost complete filling the sample bottles, they were plugged with rubber stoppers under residual water seal. Gas samples were then collected for the measurement of major components (CH_4, CO_2, N_2, O_2, H_2), He isotopes, and $\delta^{13}C$ isotopes in C-bearing gases.

Sediment samples were collected in plastic containers at the mud volcano surface for the determination of major, minor, and trace element abundance, XRD analyses, and B isotope measurements. Pore water samples were extracted from mud pulp using 50 μm mesh filters, and were then analyzed for major, minor, and trace elements as well as boron isotopes. Samples from CO_2-rich mineral waters discharged through the Tiblisi borehole in the northern foothills of the Lesser Caucasus (sample 10-97) as well as from a spring near Pchoveli mud volcano (sample 1-97) were collected for reference. All water and sediment samples were taken and stored in ultraclean plastic containers.

XRD and trace elements

The bulk mineralogy of the mud volcano sediments was determined using an automated X-ray diffractometer (Philips PW1800) at the University of Bristol, UK. X-ray diffraction patterns of smear slides were scanned from 3° to 68° 2θ at 0.02°/s, using 45 kV accelerating voltage and 30 mA current with a copper k_α source (1.5405 Å wave length). In addition, glycolated smear slides were

run from 3° to 37° to achieve a better recognition of the clay mineral phases. Additional XRD analyses were carried out on the clay fraction (<1 μm, as obtained by settling experiments and decantation) at the Geological Institute of the Russian Academy of Sciences (GINRAS). These XRD measurements of clay phases were carried out on oriented specimens (1) in natural state, (2) after glycolation, (3) after calcination at 550 °C, and (4) after 10% HCl treatment.

The chemical composition of the mud samples was determined by a combined approach of ICP-AES (major elements) and ICP-MS (minor/trace elements) at Bristol University, UK. The instruments used were a JY24 ICP-AES and a VG Elemental Plasma Quad II ICP-MS, respectively. Dried and powdered samples were digested with hydrofluoric acid, dried, redissolved in nitric acid, and then diluted for measurement. JB-1 rock standard and MAG-1 sediment standard were used to monitor the results.

Minor and trace elements of MV fluid samples were determined by inductively coupled plasma mass spectrometry (ICP-MS) at Kola Scientific Centre, Apatity (see Lavrushin et al. 1996 for details).

Helium

The mass-spectrometric determination of inert gas contents and isotopic ratios was carried out in the Kola Scientific Centre, Apatity, following the technique outlined in detail by Polyak et al. (2000). Data are reported in ppm, and as $R=^3He/^4He$ ratio. Correction of a possible contamination by atmospheric air has been carried out based on Ne or Ar (see description in Lavrushin et al. 1996).

Carbon

Contents of CO_2 and methane were determined by chromatography at GINRAS, Moscow, and at Kola Scientific Centre, Apatity. Carbon isotope ratios of gaseous carbon dioxide were carried out at the Kola Scientific Centre, Apatity (for details, see Lavrushin et al. 1996). $\delta^{13}C$ results are reported in ‰ PDB (i.e., relative to Peedee belemnite standard; see Craig 1957).

Boron

Boron concentrations of the pore fluids collected from the mud dome surface were determined by ICP-AES (JY 170 Ultratrace at GEOMAR, Kiel). Samples were diluted 1:10 with 0.5% HNO_3 prior to analysis. Boron isotope ratios of the interstitial fluids were analyzed by negative thermal ionization mass spectrometry (TIMS) on a Finnigan MAT 262 with an external precision of ±0.5‰. Owing to the low salinities of some of the MV fluids, 1 μl of boron-free seawater matrix was loaded on the filament in addition to 1 μl of sample (containing 5 ng B). Boron from sediment samples was separated after HF digestion by a series of cation and anion exchanges, following the method outlined in much detail in Deyhle (2001). Isotope ratios were collected by positive TIMS measurements at GEOMAR, Kiel (Finnigan MAT 262) with a reproducibility of ±0.13‰ ($2\sigma_{mean}$). All isotopic compositions are reported as per mil (‰) deviation from a standard (boric acid NBS SRM 951, $^{11}B/^{10}B=4.0437\pm0.0033$; Cantanzaro et al. 1970).

Results

Data of gas, water, and mud samples from a total of thirteen different mud domes are reported in the following paragraphs. The number of samples per location depended on sample availability and sample quality, so that some results are not available for each of the mud volcanoes. Some previously obtained data characterizing the same and other MVs from these regions are also included for comparison.

Mineralogy and trace elements of the mud

To shed light on mineralogical composition and possible provenance, all mud samples were analyzed by bulk X-ray diffraction (Table 1). For this reconnaissance study, relative abundance was noted only in terms of a distinction between major and minor (including trace) constituents. Special focus was directed to the clay size fraction.

The main minerals detected in all samples are quartz, kaolinite, smectite/illite and chlorite. Some specimens also have significant amounts of calcite or Mg calcite, indicating cementation due to diagenetic reactions. Illite dominates over smectite, suggesting that the majority of the marine smectite from the Kula Basin has already undergone transformation into illite (Colten-Bradley 1987). This suggests that the mudstones have experienced considerable burial (equivalent to temperatures exceeding 70–100 °C) during Caucasian orogenesis. Albite, plagioclase, or other feldspar minerals are rarely observed. Pyrite, pyroxene, kaolinite, and muscovite also occur in minor quantities. Glycolisation of the samples confirmed similarities in clay mineral composition between muds from Taman and Georgia, as expressed by abundant mixed-layer minerals of the smectite-illite group (with 30–40% of swelling interlayers) in both areas. In the Taman muds, the overall amounts of smectite are slightly higher than in Georgia, with the exception of the two southernmost volcanoes Gladkovskii and Semigorskii (Table 1). When compared to marine mud domes, the illite concentration in the Caucasus muds are approximately by a factor of 4 higher than on the Mediterranean Ridge accretionary complex where muds are dominated by kaolinite, hallyosite and smectite, but contain only traces of illite (Zitter et al. 2001).

Table 1 Bulk mineralogy results from XRD analysis on mud sediments from Georgia and Taman Peninsula. Abundance of minerals is represented by relative descending order

Mud volcano	ID	Bulk mineralogy from XRD
Georgia		
Pchoveli	2-97	Chlorite, illite, quartz, smectite, calcite, feldspar, pyrite, glauconite
Kila-Kupra	3-97	Chlorite, illite, quartz, smectite, kaolinite, calcite, pyrrhotite
Bayda	7-97	Illite, smectite, quartz, chlorite, kaolinite
Ahtala	9-97	Quartz, chlorite, illite, smectite, calcite, feldspar, muscovite
Taman		
Kuchugurski	1-94	Quartz, chlorite, illite, kaolinite, calcite, feldspar, epidote
Golubicriy	2-94	Quartz, chlorite, illite, smectite, calcite, feldspar, Mg-calcite
Polivadina	5-94	Chlorite, illite, quartz, kaolinite, smectite, muscovite, pyrrhotite
Semigorski	9-94	Chlorite, illite, quartz, calcite, feldspar, pyrite, glauconite
Gladkovski	11-94	Illite, chlorite, quartz, kaolinite, smectite, calcite, pyrrhotite
Shugo	13-94	Quartz, chlorite, illite, smectite, Mg-calcite, feldspar
Ahtanizovski	16-94	Chlorite, quartz, illite, smectite, kaolinite, calcite, feldspar, biotite
Shapurski	17-94	Chlorite, illite, quartz, kaolinite, Mg-calcite, feldspar, amphibole, glauconite
Karabetovski	25-94	Illite, quartz, chlorite, kaolinite, smectite, feldspar

Results from major, minor and trace element determination are listed in Table 2. For comparison, the average composition of global oceanic sediment (GLOSS; c.f. Plank and Langmuir 1998) is also given. The major element composition is dominated by Al_2O_3 and Fe_2O_3 (Table 2), which agrees with the finding from XRD that illite, smectite and chlorite dominate the clayey muds in addition to omnipresent quartz silt (Table 1). Concentrations of the mobile elements like Li and Cs are partly enriched relative to modern marine clays. While the latter usually range between 3549 ppm Li in marine clays (and up to 70 ppm in zones of enhanced fluid transfer; see You et al. 1995), the Caucasian MVs show values up to ~90 ppm (Georgia) and ~120 ppm (Taman; Table 2). Individual mud domes like Semigorski MV, Taman, are heavily enriched in Sr (up to ~600 ppm), Rb (up to ~160 ppm) and Ba (up to ~1300 ppm; see Table 2). MVs from both study areas show an overall enrichment in certain trace metals when compared to GLOSS (e.g., Cr, Zn, Rb, Cs; Table 2), which is very likely reflecting their affinity to clay minerals. Other trace elements are depleted in the mud, but get enriched in the fluid (e.g., Y, Ba, Pb; see next paragraph).

Chemical composition of mud volcano waters

Results for interstitial waters are presented in Table 3. If fluid composition of Georgia MV waters is compared to those from the reference borehole (sample 10-97, Table 3) and spring (sample 1-97, Table 3), it can be seen that some of the mud volcanoes show much higher concentrations for some elements. This is the case for Na, Cl (Fig. 4A), Mg (Fig. 4B), Ba (Fig. 4C), Li, Sr (Fig. 4D), B, K, Cr, Rb, and I (see also Table 3). As volatile mobilization is reflected in the focused dewatering products of the Caucasian mud volcanoes, it is expected that elements like Li and B, but also Sr and Ba are enriched in the fluids within the Caucasian orogenic wedge. This indeed is shown by Ba, Sr, Li and B, which have more than one order of magnitude higher concentrations than seawater in certain MVs (Table 3). Moreover, the strong enrichment in Ba (samples 2-97, 3-97, 9-94 and 13-94) indicates that the muds originate in an anoxic, sulfate-free environment. A comparison between the two areas is difficult because of the variability between the fluids from the individual mud volcanoes. There are, however, some significant differences, like stronger freshening of the Taman waters in the Greater Caucasus when compared to Georgia (see e.g., salinity, Na, and Cl in Table 3). Also, many of the other elements analyzed in both sample sets indicate higher concentrations in Georgia. For instance, a significant enrichment is found for Sr (average 436 μM [Georgia] and 116 μM [Taman] compared to 87 μM in seawater) and Li (338 μM [Georgia] and 409 μM [Taman] compared to 27 μM for seawater), respectively (Fig. 4D and Table 3). Having profound pore water freshening, on the one hand, and presumably secondary diagenetic processes causing a strong enrichment of some mobile elements (without necessarily enhancing chlorinity or salinity drastically), on the other hand, will be discussed below.

There are also interesting variations between the individual mud cones. Like in the Georgia muds (see above and Table 2), Ba is heavily enriched in the Georgian MV waters and even in the adjacent spring. Compared to modern seawater with a concentration of 0.45 μM, the average Ba content in both the MV fluid series varies between an average 41 μM [Taman] and 186 μM [Georgia] (Table 3). As expected, the fluids show an increase in Ba when sulfate concentrations decrease (see Fig. 4C). It appears that a threshold value of 50 μM SO_4 or lower, allows Ba to be preserved at high concentrations (as seen for samples 2-97 and 3-97). Mobilization of Ba in marine sediments occurs easily when these low levels of dissolved sulfate appear (Brumsack and Gieskes 1983; von Breymann et al. 1992). This observation also points toward a significant difference regarding the fluid source between these two MVs and their counterparts (samples 7-97 and 9-97). In addition to Ba (Fig. 4C), Mg, Ca (Fig. 4B), and Sr (Fig. 4D) are enriched in Pchoveli and Kila-Kupra MVs

Table 2 ICP-AES results (major elements) and ICP-MS results of mud samples taken at Georgia (2-97 through 9-97) and Taman Peninsula (1-94 through 25-94)

	Georgia				Taman Peninsula									Averaged concentrations			Normalized concentrations	
	2–97	3–97	7–97	9–97	1–94	2–94	5–94	9–94	11–94	13–94	16–94	17–94	25–94	Georgia	Taman	GLOSS	Ratio Georgia/ GLOSS	Ratio Taman/ GLOSS
	Wt%	Wt%	Wt%	Wt%	Wt%	Wt%	Wt%	Wt%	Wt%	Wt%	Wt%	Wt%	Wt%	Wt%	Wt%	Wt%		
TiO_2	0.42	0.59	0.33	0.27	0.80	0.71	0.43	0.66	0.69	0.70	0.69	0.81	0.74	0.40	0.69	0.62	0.65	1.12
Al_2O_3	12.95	13.16	11.82	14.77	14.64	14.05	6.86	14.97	14.73	13.39	14.05	14.14	5.79	13.18	12.51	11.91	1.11	1.05
Fe_2O_3	3.59	8.41	4.29	6.05	7.34	6.44	4.30	6.12	6.59	4.92	6.55	6.66	6.29	5.59	6.14	5.21	1.07	1.18
MnO	0.07	0.15	0.04	0.01	0.08	0.11	0.12	0.10	0.08	0.06	0.08	0.12	0.14	0.07	0.10	0.32	0.21	0.31
MgO	2.15	1.99	0.55	1.06	1.92	1.82	0.10	1.68	1.95	1.40	2.00	2.01	0.22	1.44	1.46	2.48	0.58	0.59
CaO	2.56	3.47	1.52	0.83	1.23	3.76	0.21	3.53	3.53	3.57	3.58	1.85	0.44	2.10	2.41	5.95	0.35	0.41
Na_2O	1.65	1.48	0.93	0.88	1.51	1.45	0.97	1.59	1.53	1.25	1.40	1.94	1.24	1.23	1.43	2.43	0.51	0.59
K_2O	2.01	1.19	1.07	2.24	1.74	1.89	1.39	1.27	1.31	2.11	2.02	2.02	1.74	1.63	1.72	2.04	0.80	0.84
P_2O_5	0.12	0.07	0.17	0.08	0.14	0.13	0.08	0.17	0.17	0.10	0.14	0.14	0.14	0.11	0.13	0.19	0.59	0.71
	ppm	ppm	ppm	ppm	ppm	ppm	ppm	ppm	ppm	ppm	ppm	ppm	ppm	ppm	ppm	ppm		
Li	91.21	31.00	15.53	113.91	65.78	48.22	37.34	75.91	123.18	97.37	52.13	62.34	25.22	62.91	65.28	–	–	–
Be	0.10	0.35	1.20	0.70	1.60	2.39	1.84	0.94	2.89	3.52	1.78	1.31	1.41	0.59	1.97	–	–	–
Cr	51.20	82.93	108.80	149.11	128.55	131.55	71.44	81.87	148.25	122.18	124.46	131.24	78.21	98.01	113.08	79.04	1.24	1.43
Zn	127.26	133.50	71.35	68.71	117.92	115.98	79.65	93.88	105.73	90.50	84.76	119.84	90.92	100.20	99.91	86.33	1.16	1.16
Rb	106.51	98.08	26.38	38.29	67.00	81.51	62.99	90.63	164.96	84.20	74.16	73.88	107.89	67.32	89.69	57.26	1.18	1.57
Sr	486.20	601.85	28.88	45.89	126.92	214.03	15.90	532.07	155.35	358.31	198.24	267.54	107.07	290.71	219.49	329.38	0.88	0.67
Y	3.22	21.14	4.10	2.20	15.53	19.06	0.38	15.89	14.64	15.79	18.07	18.92	1.09	7.66	13.26	30.23	0.25	0.44
Cs	8.78	31.20	26.47	4.79	5.34	5.74	0.80	6.02	40.34	7.94	5.96	5.83	0.53	17.81	8.72	3.46	5.15	2.52
Ba	1039.11	1213.81	105.09	474.52	374.40	402.65	53.81	1296.25	441.41	1065.03	376.33	652.00	85.87	708.13	527.53	775.75	0.91	0.68
Pb	4.49	16.12	7.08	5.81	21.18	18.24	12.00	14.86	20.08	18.81	18.99	21.67	6.90	8.37	16.97	19.87	0.42	0.85
Th	0.21	13.55	2.26	1.62	13.10	14.50	0.23	15.97	19.89	16.02	15.27	16.04	0.90	4.41	12.44	6.96	0.63	1.79
U	0.84	1.75	2.20	1.56	2.59	2.05	0.98	2.05	2.30	1.73	1.69	2.30	1.93	1.59	1.96	1.67	0.95	1.17

Table 3 ICP-MS results of four mud volcano interstitial waters, a spring (sample 1–97) and water from a reference drillhole (sample 10–97) in Georgia (for location, see Fig. 1). Data from Taman Peninsula MVs are taken from Lavrushin et al. (1996). Data for some elements are missing, because no Taman fluids were available for this study

	Georgia						Taman Peninsula								Averaged concentrations			Normalized concentrations	
	1-97 Spring	2-97 Pchoveli	3-97 Kila-Kupra	7-97 Bayda	9-97 Ahtala	10-97 Ref. bore-hole	1-94 Kuchu-gurski	2-94 Golu-bicriy	5-94 Poli-vadina	9-94 Semi-gorski	11-94 Glad-kovski	13-94 Shugo	17-94 Sha-purski	25-94 Kara-betovski	Georgia	Taman	Seawater	Georgia	Taman
Na (mM)	102	541	433	227	263	3	182	180.1	184	124.9	253.9	267.8	242.1	150.2	366	198.1	480	0.76	0.41
Cl (mM)	195	680	549	199	270	3	126	194	76	46	338.1	230.1	168.0	80.0	425	157.3	559	0.76	0.28
Salinity	14	40.5	34	14	18.5	0.5	11.6	12.1	–	9.2	22.5	19.2	15	10.3	26.8	12.5	42	0.64	0.30
I (μM)	7.2	7.5	12.3	10.8	6.3	–	37.1	n.a.	24.5	2.9	2.2	2.2	17.1	9.6	9.2	13.7	n.a.	n.a.	n.a.
SO_4 (mM)	0.04	0.05	0.08	2.5	0.09	0.08	1.6	0.2	0.02	0.56	0.04	0.17	0.26	0.1	0.7	0.37	28.9	0.02	0.01
K (mM)	n.a.	1.28	0.91	0.13	3.35	n.a.	1.6	2.6	2.7	1.0	7.7	3.6	1.7	1.2	1.4	2.7	10.44	0.14	0.26
Li (μM)	6	462	166	64	662	3	95.0	n.a.	93.0	116	1234	1116	83	123.0	338.5	408.6	27	12.54	15.13
B (mM)	0.04	3.51	1.8	5.62	10.43	0.36	14.8	n.a.	7.4	28.6	20.5	44.8	8.4	26.2	5.3	21.5	0.42	12.71	51.19
Ca (mM)	27.98	9	10.45	0.18	0.79	0.06	2.0	2.7	1.4	2.3	36	2.5	1.6	0.8	5.1	6.2	10.55	0.48	0.58
Mg (mM)	6.21	10.53	12.2	1.23	3.68	n.a.	2.5	8.4	2.9	0.4	3.2	3.5	1.6	1.3	6.9	3	54	0.13	0.06
Ba (μM)	74.8	329	379	3.8	31.1	0.1	0.3	n.a.	6.3	47.6	66.6	154.2	7.6	7	185.7	41.4	0.45	412.72	92.00
Sr (μM)	568	622	948	56	117	1	100.2	n.a.	18	48.8	420.8	183.6	21.4	21	435.8	116.3	87	5.01	1.34
Cr (μM)	0.11	0.07	0.12	0.4	0.22	n.d.	0.17	n.a.	0.04	0.04	0.08	0.08	0.08	0.04	0.20	0.076	0.005	40.50	15.20
Rb (μM)	0.07	0.14	0.3	0.09	0.11	0.02	0.11	n.a.	0.19	0.15	8.46	0.69	0.06	0.14	0.16	1.4	1.4	0.11	1.00
Y (μM)	0.012	0.005	0.097	0.005	0.006	n.d.	0.009	n.a.	0.002	0.002	0.004	0.004	0.004	0.002	0.028	0.004	0.003	9.42	1.33
Cs (μM)	0.002	0.002	0.004	n.d.	n.d.	0.003	0.002	n.a.	0.001	4.35	0.017	0.001	0.002	0.002	0.003	0.63	0.004	n.a.	157.50
U (μM)	n.d.	0.005	0.01	0.015	0.008	n.d.	0.726	n.a.	0.001	0.001	0.003	0.006	0.001	0.014	0.010	0.11	0.013	0.73	8.46
Th (μM)	n.d.	0.002	0.001	0.001	n.d.	n.d.	0.001	n.a.	n.d.	0.001	0.001	n.d.	0.001	n.d.	0.001	0.001	0.0002	n.a.	5.00

n.a.,not analyzed; n.d.,not detected

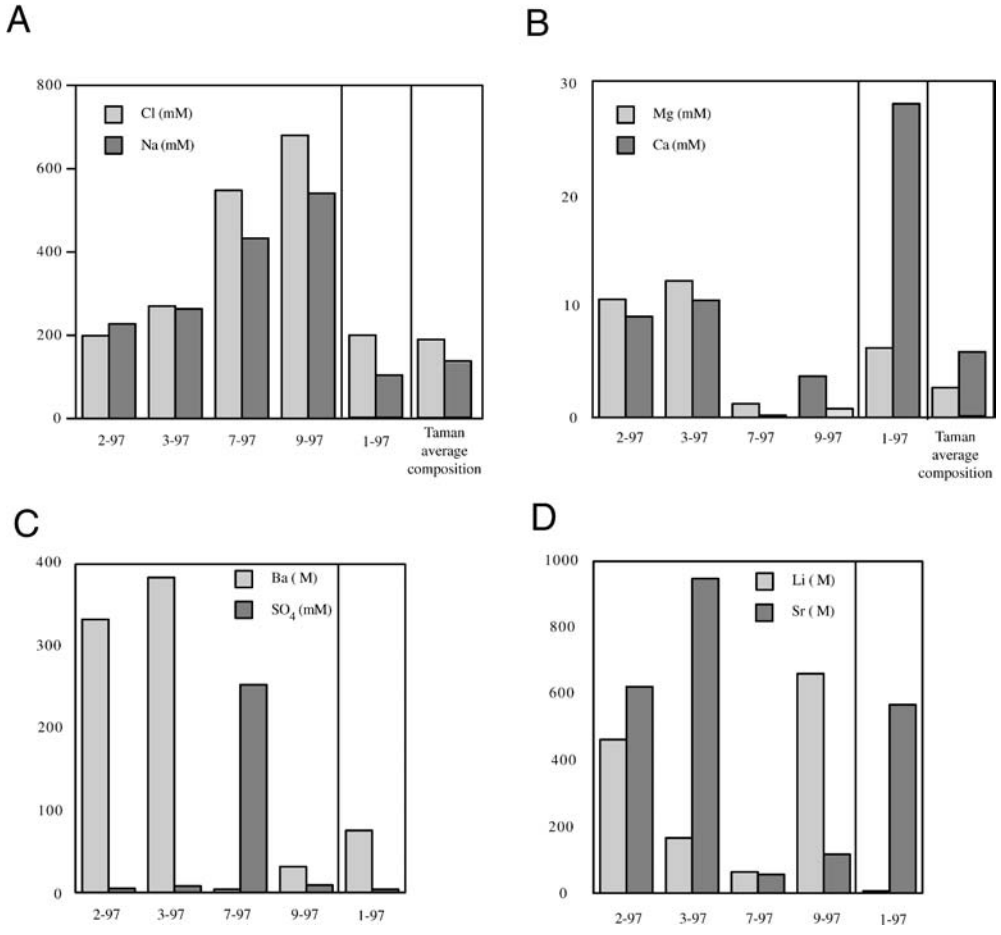

Fig. 4 Results from ICP-MS on mud volcano fluids from Georgia (see also Table 3). **A** Na, Cl; **B** Ca, Mg; **C** Ba, SO_4; **D** Sr, Li. Note the differences between mud volcanoes 2-97 and 3-97 on one hand and 7-97 and 9-97 on the other hand; 1-97 is the spring on Pchoveli mud volcano for reference. Average contents of Na, Cl, Ca and Mg from Taman mud volcano waters are plotted in **A** and **B** for comparison. For full set of results refer to Table 3

(samples 2–97 and 3–97), while Na, Cl (Fig. 4A), SO_4 (Fig. 4C), B and I are enriched in Bayda and Ahtala MVs (7-97 and 9-97). The observed variations suggest a different fluid origin, and possibly even a different reservoir of liquefied mud, for individual mud domes. In the discussion, we relate our results to the complex tectonic framework and possible mechanisms of fluid generation. Similarly, the Taman fluids show strong variations between individual domes (Table 3). Gladkovski MV shows the strongest enrichment in the majority of the elements, in some cases reaching concentrations which exceed those of teh Taman average value by a factor of 3–4 (e.g., Li, Rb, Sr; Table 3). Other features, like Karabetovski or Semigorski MVs lie generally below the regional average. Since there is no systematic difference in style of mud eruption or size of the dome, our contention is that fluid flow along deep-seated faults is hindered in some places, but favoured in others (at least on a temporary basis).

If the fluid geochemistry of the two study areas are compared, a more systematic pattern is observed. Since freshening due to clay mineral processes may be stronger in pore waters from the more illite-rich Taman muds, many of the elements are depleted. Not only are salinity, Na, or Cl much lower in Taman (approx. half the Georgia values; Table 3), but Ca, Sr, Mg and Ba are also significantly diluted. By contrast, the mobile phases like B, Li as well as elements generally adsorbed to clay minerals (U, Cr) are enriched in Taman where deformation and dewatering are assumed to be stronger. We will address this aspect in the discussion.

Helium in mud volcano gases

Results from helium analyses carried out on eleven MV gas specimens and the reference borehole in Georgia are presented in Fig. 5. The MV gas samples show a variation in He over more than two orders of magnitude (i.e., 3872 ppm; see Table 4 and Lavrushin et al. 1996). As with the aqueous fluids, this result suggests that the amount and type of gas associated with each mud dome may vary considerably. Although there is no clear distinction between the He contents in Taman and Georgia, we find significant differences in the He isotope ratio between the two study areas (Fig. 5 and Table 4). The $^3He/^4He$ isotope ratio of the Taman samples ($R=2.816\times10^{-8}$, Table 4) corresponds to radiogenic helium generated in terrestrial rocks, whereas gases from Georgian MVs as well as from the reference borehole (sample 10-97) range approximately one order of magnitude higher ($R=30200\times10^{-8}$; see Table 4).

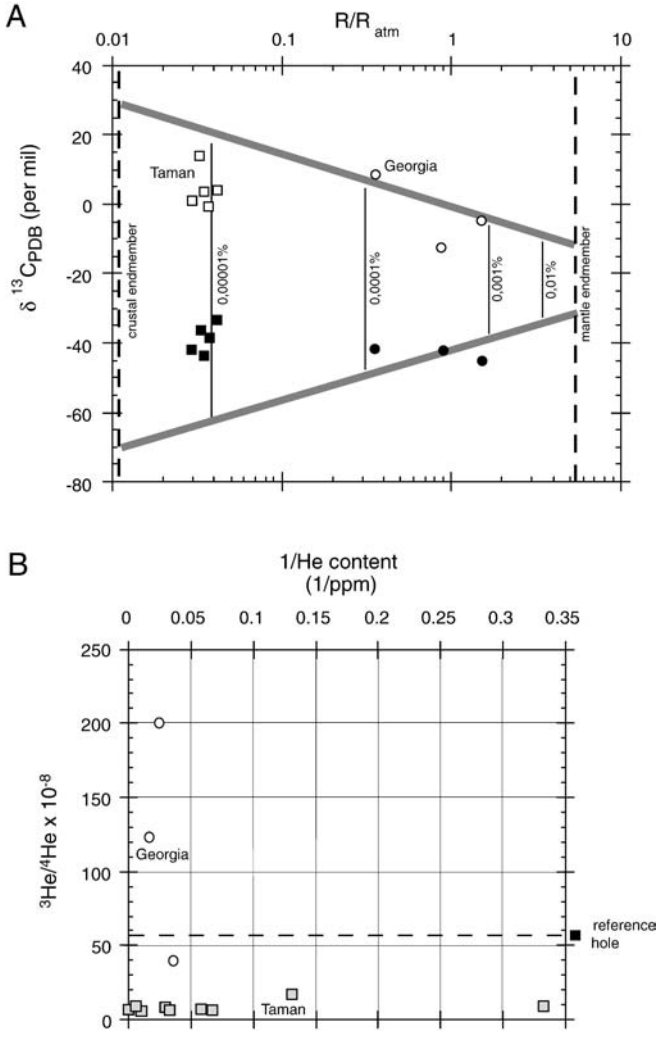

Fig. 5 **A** $\delta^{13}C$ from CH_4 and from CO_2 vs. R/R_{atm} of He gas from the mud volcanoes in Georgia (*circles*) and the Kerch-Taman Peninsula (*squares*). *Solid symbols* are methane, while *open symbols* represent CO_2. The two *subhorizontal lines* represent the trend of two-end member-mixing between terrestrial/crustal rock (on the left) and mantle material (*dotted vertical line* at the right; cf. Jenden et al. 1993). The percentage along the subhorizontal lines indicates the inferred mantle contribution. **B** He isotope ratio (R/R_{atm}) vs. 1/He content (in 1/ppm) from gases from Georgia mud volcanoes (*open circles*) and Taman mud volcanoes (*squares*). The *dashed line* represents the R/R_{atm} value in the reference borehole in Georgia where no He content could be measured

Given that helium isotope ratios are approximately $R=1.4\times10^{-6}$ in the atmosphere (Mamyrin et al. 1970), and $R=1.2\times10^{-5}$ in the mantle (Mamyrin and Tolstikhin 1981), the input of "light" ^3He into the MV samples can be quantified. Possible explanations for the observed R-values are (1) admixture of gas from lower crustal or mantle depth, or (2) the high Li-content of the surrounding rocks (as well as the mud; see Table 2), which may cause high concentrations of ^3He and hence affect the radiogenic He isotope ratio (Andrews 1985). Using a two end-member mixing model (Jenden et al. 1993), we estimated the input of He of presumed mantle signature to be as little as 0.00001% at Taman, and up to around 0.001% in Georgia (Fig. 5A, grey bars). Despite rather small amounts of total gas volume, these numbers differ by two orders of magnitude in potential mantle helium between Georgia and Taman. The difference is also apparent when the reciprocal He content is plotted versus the He isotope ratio. As illustrated in Fig. 5B, the Taman MVs plot almost entirely along the x-axis, while the gas from Georgia mud domes appears aligned vertically. The most obvious explanation for such a finding would be the different structural style in the two areas, as is discussed below.

Carbon isotopes and C-bearing gas contents

Methane is the dominant mud volcano gas phase in Georgia and Taman, ranging from about 70%vol to more than 99%vol in places (Table 4). CO_2 concentrations are generally low (less than 15%vol), or even not detectable. The only exception is Kuchugurski MV near the Sea of Azov coast, where 29%vol were measured (Table 4; Fig. 1, inset 1 for location of the feature). Higher hydrocarbons occur in negligible amounts, i.e., ethane <<0.5%vol, and propane <<0.005%vol (see Lavrushin et al. 1996).

When the entire set of carbon isotope ratios ($\delta^{13}C_{PDB}$) is considered by itself, no clear distinction can be made between the Taman and Georgia MVs. Although $\delta^{13}C$ values from CO_2 and CH_4 differ considerably (Fig. 5A), Taman and Georgia gas samples plot in the same respective range. Only when contrasted with He isotope data, do samples from the two MV areas plot as separate groups (Fig. 5A). Carbon isotope data of −19.4 to 13.5‰ from this study agree well with earlier data from mud domes nearby (−36.9 – 23.4‰; Valayev et al. 1985). They are significantly more positive than the respective $\delta^{13}C$ from methane, which range between −33 and −49‰ (Table 4).

Boron and boron isotopes in mud and fluids

Boron contents of pore fluids and muds from the different MVs are shown in Table 4 and Fig. 6. Boron concentrations range from 1.810.6 mM in fluids and from ~144–323 ppm in the mud of Georgian MVs. In contrast, B contents of fluids from the reference drillhole and the spring on Pchoveli MV are more than two orders of magnitude lower (0.04 mM; see grey shading in Table 4). In Taman, B contents are 2.5 – 14.9 mM in the fluids, and from ~143–868 ppm in the muds. This shows that both fluids and muds of the Taman MVs have higher B concentrations. B concentrations of MV waters are spectacularly high compared to hydrothermal fluids (0.5 – 0.6 mM; cf. Spivack 1986), and also to pore fluids from other mud volcano localities (see discussion below). Similarly, B contents in the mud are significantly higher than those from marine sediments studied previously

Table 4 CH_4, CO_2, He and B concentrations and He, C, and B isotope ratios for MV samples from Georgia and Taman. Right column shows mobilization depth estimates of the Taman mud from an earlier study by Lavrushin et al. (1996) which are used in Fig. 8

Sample ID	Ref no. in Fig. 1, and in Lavrushin et al. (1996)	Name of MV	He content (ppm)	R/R_{atm} ($^3He/^4He \times 10^{-8}$)	CH_4 content (%vol)	$\delta^{13}C$ (CH_4)	CO_2 content (%vol)	$\delta^{13}C$ (CO_2)	B contents (fluids in mM; mud in ppm)	$\delta^{11}B$ (‰)
Georgia:										
Fluid:										
1-97	–	Spring Pchoveli	–	–	–	–	–	–	0.04	23.2
2-97	–	m.v. Pchoveli	–	–	–	–	–	–	3.6	36.6
3-97	33	m.v. Kila-Kupra	30	200	–	–48.9	–	–3	1.8	39.2
7-97	35	m.v. Bayda	10	30	–	–42.3	–	11.3	5.7	38.4
9-97	32	m.v. Ahtala (Gurdjaani)	50	122	–	–43	–	–9.8	10.6	22.5
10-97	40	bh. Tbilisi-Lisi	–	56	–	–	–	–	0.04 (av. 5.4)[a]	26.5 (av. 34.2)[a]
Mud:										
2-97	–	m.v. Pchoveli	–	–	–	–	–	–	248.0	5.1
3-97	33	m.v. Kila-Kupra	–	–	–	–	–	–	143.6	0.1
7-97	35	m.v. Bayda	–	–	–	–	–	–	256.2	7.4
9-97	32	m.v. Ahtala (Gurdjaani)	–	–	–	–	–	–	323.0 (av. 243)	–1.2 (av. 2.825)
Taman Peninsula:										
Fluid:										
1-94	1	m.v. Kuchugurski	3.05	7.4	69.9	–	29.2	–	4.9	26
2-94	2	m.v. Golubicriy	13.7	2.8	91.8	–	0	–	–	–
5-94	4	m.v. Polivadina	16.5	4	85.8	–	13.1	–	2.5	23.7
9-94	5	m.v. Semigorski	120–204	5.3–6.3	94.8	–38.5	3.4	–0.5	9.5	16.5
11-94	6	m.v. Gladkovski	872	4.8	94.2	–33.4	0	4	6.8	35.4
13-94	8	m.v. Shugo	22.5–35.4	3.8–4	89.5	–41.4	8.5	2.1	14.9	27
16-94	11	m.v. Ahtanizovski	103	5.3	82.5	–43.5	14.4	3.8	–	–
17-94	12	m.v. Shapurski	7.7	16	92	–	6.7	–	2.8	32.6
25–94	19	m.v. Karabetovski	30–34	3.9–6	99.1	–36.7	0.3	13.5	8.7 (av. 5.9)	42.4 (av. 29.1)
Mud:										
1-94	1	m.v. Kuchugurski	–	–	–	–	–	–	339.1	3.8
2-94	2	m.v. Golubicriy	–	–	–	–	–	–	328.6	–1.5
5-94	4	m.v. Polivadina	–	–	–	–	–	–	316.5	1.4
9-94	5	m.v. Semigorski	–	–	–	–	–	–	538.8	–4.4
11-94	6	m.v. Gladkovski	–	–	–	–	–	–	280.2	–6.1
13-94	8	m.v. Shugo	–	–	–	–	–	–	421.8	–7.7
16-94	11	m.v. Ahtanizovski	–	–	–	–	–	–	868.1	–0.5
17-94	12	m.v. Shapurski	–	–	–	–	–	–	366.8	7
25-94	19	m.v. Karabetovski	–	–	–	–	–	–	142.6	2.4

[a] Spring and borehole fluids have not been included in mean average calculations

(Ishikawa and Nakamura 1993). While average B content of the mud exceeds that of marine sediments by a factor of 24, maximum values in Taman are 8× higher than in marine clays. The fact that both fluids and muds in either area are enriched relative to seawater and marine clays, respectively (i.e., no complementary enrichment-depletion pattern exists) suggests that their boron originates from different sources (see discussion). The $\delta^{11}B$ isotopes of the Taman and Georgia muds show a wide scatter from approximately −8 to +7‰ (Table 4; Fig. 6). Such isotope ratios agree in broad terms with those of modern marine sediments, especially when these sediments contain significant amounts of smectite (+2.3 to +9.2‰) or detrital illite (−13 to −8‰; see Ishikawa and Nakamura 1993). On the other hand, low $\delta^{11}B$ signatures are generally believed to indicate a preferential removal of ^{11}B from the mud during diagenetic reactions (You et al. 1995), recrystallization, or in the course of smectite–illite transition (Ishikawa and Nakamura 1993). The fluid B isotope ratios range from 22.5 to 39.2‰ in Georgia and 16.5 to 42.4‰ in Taman (Table 4). On average, the Taman MVs have lower$\delta^{11}B$ (29.1‰) compared to Georgia (34.2‰). The measured $\delta^{11}B$ ratios are generally lighter than that of seawater (39.5‰), and are hence depleted in heavy ^{11}B. Consequently, because both $\delta^{11}B$ of the fluids and muds are lighter than the initial seawater and clay ratios further supports the contention that they originate from different sources (see discussion).

If we compare the B isotope trends of two study areas, there is a subtle difference in $\delta^{11}B$ in the muds, with the

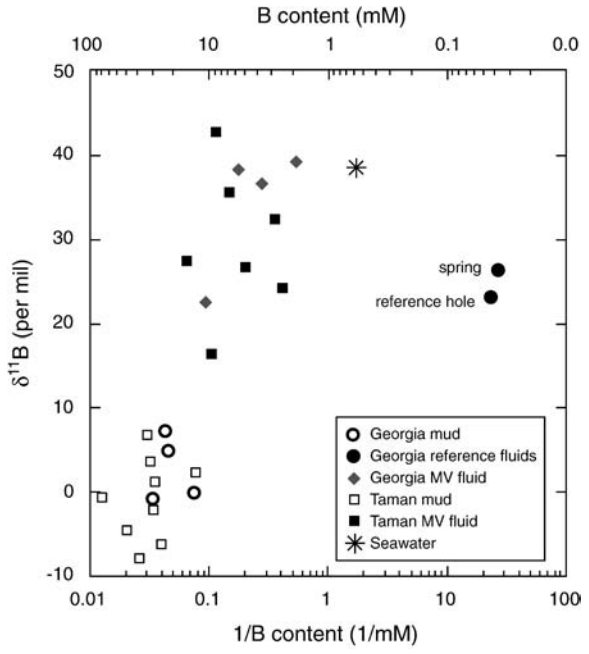

Fig. 6 δ^{11}B vs. 1/B content of mud volcano samples from Georgia (including the reference borehole and spring) and Taman Peninsula. Note that all sediment data have been converted into molar concentrations to allow a comparative cross-plot

average value in Georgia (2.8‰) being slightly higher than that in Taman (–0.9‰; see data in Table 4). Given the scatter of the individual mud measurements (Fig. 6), however, the significance of this difference of ~3.7‰ is difficult to assess. Assuming a similar initial composition in either area, our results suggest that more desorbable B has been released from the Taman muds. On the other hand, preferential removal of adsorbed B from the mud is in conflict with its high remaining B contents (see above), so that a more complex explanation is required (see discussion below).

Discussion

In this paper we try to answer the following two questions in the basis of our results: First, to which extent are the chemical and isotopic signatures indicative of the mobilization depth (i.e., P–T regime) of the gaseous, aqueous, and solid extruded phases? Second, how does the combined geochemical evidence fit into the overall picture of devolatilization, liquefaction, and extrusion mechanics within the regional tectonic framework?

Mobilization depths of fluids and mud

As solid, aqueous, and gaseous phases of the mud volcanic ejecta may originate from different sources, or reservoirs, we split the first part of the discussion into three parts.

Gas

The majority of the mud volcanoes comprise methane as the dominant gas, in places reaching almost 100%vol (Table 4). Methane has been demonstrated to generally exceed 95%vol of the total amount of mud volcano gas (e.g., Limonov et al. 1995; Kopf et al. 1998). In general, the methane data from the limited number of Georgia mud volcano specimens cover the same range of δ^{13}C compositions as the samples from Taman mud volcanoes (Fig. 5). However, there appears to be a regional variation in methane origin, with predominantly biogenic δ^{13}C signatures in marine environments and thermogenic methane (and higher hydrocarbons) emitted from continental mud volcanoes. In this study, $\delta^{13}C_{(CH4)}$ ratios of −33.4 to −62.8‰ lie well within the field of thermogenic methane (e.g., Vinogradov and Galimov 1970). Thermogenic methane originates from approximately 2–4 km depth (where highly reflective patches in 3D seismic data have been associated with gaseous mud reservoirs (Cooper 2001), or deeper. However, recent work on rocks from the western Canadian Basin suggests that thermogenic hydrocarbons may form at temperatures as low as ~60 °C. The methane is the result of maturation of organic matter in the sedimentary rock, and hence is strongly linked to the thermal regime, but not primarily to the tectonic framework. The slight variations found between individual mud domes are best explained by differences in mobilization depth of the gases (Prasolov and Lobkov 1977).

Although less abundant than methane, carbon dioxide also occurs in substantial amounts (Table 4). For $\delta^{13}C_{(CO2)}$, a range from about −13‰ to +13‰ is found in either area (Table 4). Such $\delta^{13}C_{(CO2)}$ signatures may be interpreted to indicate an origin of "metamorphogenic" crustal levels (−10 to −4‰), "juvenile" (−4 – 10‰), and "ultraheavy" (>10‰) degassing products of the mantle (see discussion in Valyaev et al. 1985; Lavrushin et al. 1996). While some of the CO_2 may originate from a shallow source, the "heavy" $\delta^{13}C_{(CO2)}$ of suggested metamorphogenic origin, with the "ultraheavy" end-members pointing towards deep crustal levels (Lavrushin et al. 1996). The widely known presence of "ultraheavy" CO_2 generation accompanying methane formation at shallower levels (see Whiticar 1999) can be envisaged as an alternative explanation for the isotope ratios observed in the Caucasus.

In addition to the carbon isotopes, high δ^3He (R) ratios are good indicators for a deep-seated gas component, possibly from a crustal or mantle level (Polyak et al. 1976). In the study area, anomalously high helium isotope ratios of $R=2\times10^{-6}$ have previously been explained to originate from the presence of magmatic melts in the mantle, most likely associated with the Neogene-Quaternary volcanic activity in the Greater and Lesser Caucasus (Lavrushin et al. 1996). However, the mantle component traced is estimated to be as little as 0.001% in the Georgia mud domes, and another two orders of magnitude lower at Taman (0.00001%). We propose that the higher R values

of the Georgian mud volcanoes indicate a deep source, with gas migrating along NE-vergent, deep-seated faults related to the collision of the indenting Dagestan block (Figs. 1, 2). The contribution may be episodic, possibly as a function of fault movement within the imbricate thrust stack (namely northeast of the Kura region; Fig. 2). Gas as well as waters from metamorphic reactions may then migrate upwards along fissures and microfaults, and subsequently they accumulate in certain reservoirs (at depth of mud mobilization; cf. Cooper 2001), and trigger extrusion of the buoyant mud.

Pore waters

There are several depth-indicative processes indicated by our pore fluid results. First, both the Taman and, to a lesser extent, the Georgia fluids have salinities and chlorinities considerably lower than seawater (~30–40% in Taman, and ~70% in Georgia; Table 3). This suggests that the original interstitial water in the Caucasian sedimentary rocks has been freshened by mineral dehydration reactions. Such processes initiate at intermediate depths, at temperatures as low as 70–100 °C. Among the most prominent processes are opal-quartz reactions (Ernst and Calvert 1969), illite–smectite transformation (Colten-Bradley 1987), tectonic compaction (Fitts and Brown 1999), or diagenetic and metamorphic reactions, the latter of which cover a wide range of pT conditions (e.g., Moore and Vrolijk 1992). These processes occur discontinuously within the sedimentary succession, or even the crust, which has approximately 8% hydrous minerals in its upper part (Kastner et al. 1991). In the Caucasian mudrocks, clay mineral dehydration is probably the most important of the abovementioned phenomena. With increasing temperature and stress (of the overburden as well as due to tectonic shortening), smectite interlayer water as well as water from diagenetic transformation to illite is expected to lower the salinity (Moore and Vrolijk 1992).

In addition to the different degree in interstitial water freshening (see above and Table 3), the sodium to chloride ratios in the two study areas are remarkably different. While the Georgian fluids contain more Cl than Na, Taman fluids show lower chlorinity and higher sodium (Table 3). When Na/Cl is plotted against chlorinity, the Taman waters from the Greater Caucasus plot subvertically in the left part of the diagram, showing the highest Na/Cl ratios when compared to other deep-seated mud volcano fluids from elsewhere (see caption of Fig. 7A). By contrast, the Georgian fluids plot subhorizontally at a relatively low Na/Cl ratio around 1, which is similar to the Barbados mud volcanoes (Martin et al. 1996). Given that the latter features have been suggested to originate from only 2–3 km depth (Kopf 2002), the distinct differences between Taman and Georgia in Fig. 7A are a hint towards a different evolution and mobilization depths in the two areas studied.

Despite the pore water freshening in some major constituents, some volatile species show the opposite behavior. Mobile elements like Sr, Ba, and Li in the fluids show remarkable enrichment despite the overall decrease in salinity (Table 3). Release of these elements as a result of diagenetic reactions during compaction and transformation has probably caused the high element concentrations in the pore waters. Consequently, these geochemically mature fluids may originate from a depth greater than the actual intermediate reservoir of liquefied mud (2–4 km; Cooper 2001) where temperature-driven devolatilization is more accentuated.

Boron contents in the fluids mirror those of Li and Ba, with maximum enrichment to approximately 35x seawater. Isotope values further suggest that this mobilization of B was accompanied by fractionation. As for the B isotope geochemistry, our working hypothesis is that the desorbable, trigonal ^{11}B species gets enriched in the fluid phase and depleted in the sediment with increasing depth, mostly owing to B desorption from the mud (e.g., You et al. 1996a, 1996b). The adsorbed B has been shown to have isotope ratios of ~15‰ (Spivack et al. 1987). Hence, one would expect a "deep" fluid to be characterized by heavy isotope ratios and high B contents. Both can be observed in the Caucasus MV waters (Table 4). The entire suite of $\delta^{11}B$ are less than the modern seawater value (39.5‰; Palmer and Swihart 1996), with a depletion to values as low as 22.5‰ (Figs. 6, 7B). Given the decrease in salinity as well as the B enrichment of the mud, the enrichment in B in the Georgian MV fluids up to 10.6 mM is surprising. On the other hand, it agrees well with other mud volcano areas onshore and offshore. Enrichments in B are common in mud volcanoes. For instance, in Trinidad, mud volcano waters reach 0.31 – 11.86 mM B (Dia et al. 1999), in Taiwan waters B scatters between 0.16 – 9.95 mM (Gieskes et al. 1992), and on the Mediterranean Ridge, B in pore waters ranges from 0.1 – 61 mM (Deyhle and Kopf 2001). The Georgian data also correspond with thermal saline waters from mud volcanoes of the Black Sea area (Lagunova 1976), where B in some brines reaches up to 85 mM (i.e., >200× seawater). The elevated boron concentrations have previously been correlated with increasing bicarbonate concentrations, but more importantly seem to relate to loss of desorbable boron (dominantly ^{11}B) from clay minerals into the fluid (e.g., You et al. 1996b). In addition, above ~100 °C, B can be released from the sediment matrix though diagenetic reactions (You et al. 1996a, 1996b). However, especially this latter process would cause B removal from the mud, which is not observed in an open system like the Caucasian muds (see below, and Table 4).

Most interestingly, not only mobile elements have been released into the mud volcano fluids. For example, many of the elements presented in this study (Table 3) have been long known to be enriched in volcanic arc magmas of subduction zones (relative to an upper mantle source; Plank and Langmuir 1998). These include K, Ba, Sr, Rb, Cs, but also rare elements like U, Th or Y. Although these elements are recycled in the arc, a

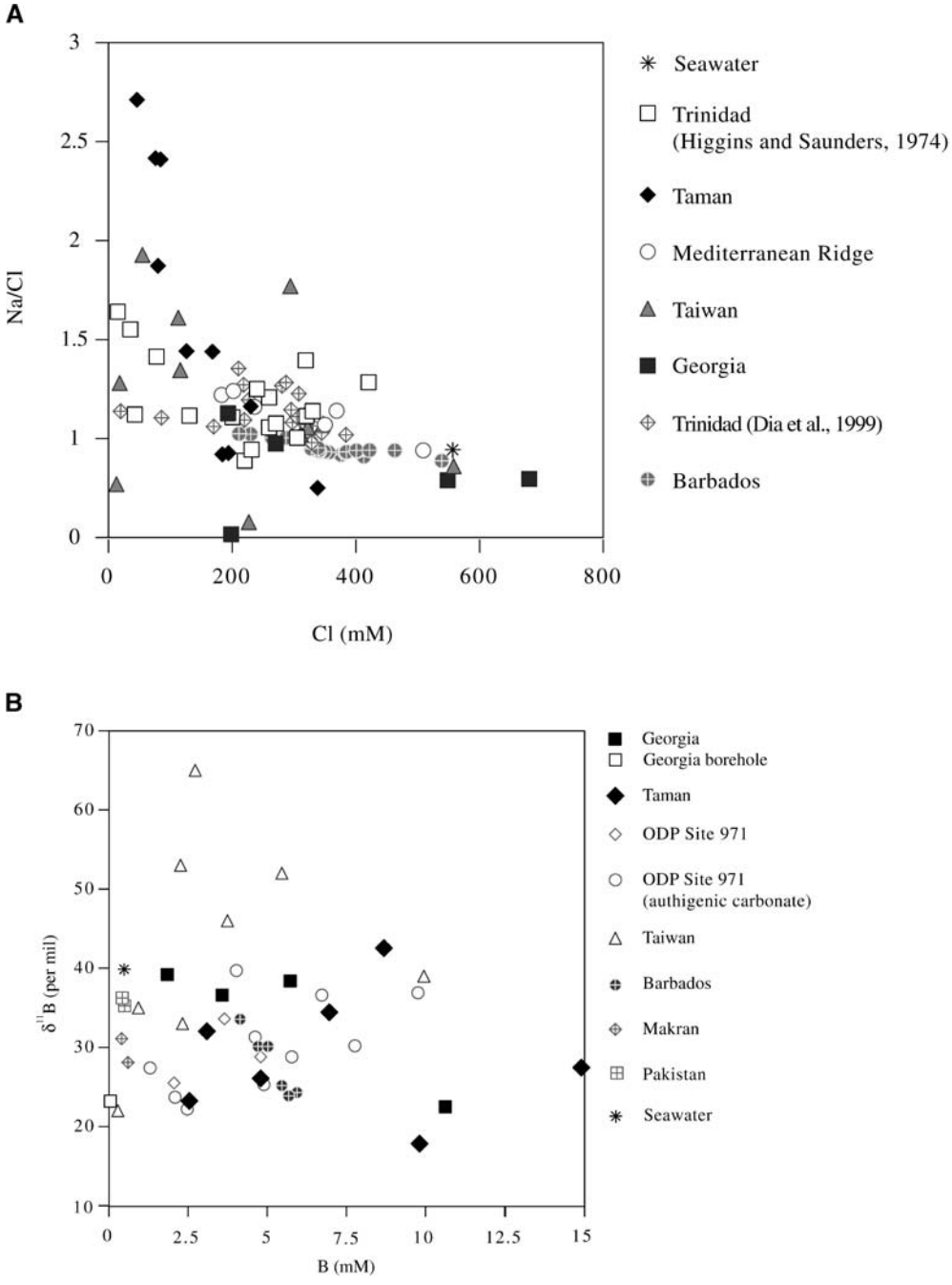

Fig. 7 **A** Comparison of Cl content vs. Na/Cl ratio in mud volcano waters from onshore and offshore examples; **B** comparison of B content vs. $\delta^{11}B$ from mud volcanoes in the Caucasus and elsewhere. For complete data reference, see Barbados Ridge: Martin et al. (1996), Taiwan: Gieskes et al. (1992), Trinidad: Higgins and Saunders (1974), Dia et al. (1999), Mediterranean Ridge: Deyhle and Kopf (2001), and Taman Peninsula: Lavrushin et al. (1996)

considerable proportion of the initial sediment input has been demonstrated to be released to the fluid in hydrothermal experiments up to only 70 MPa stress and temperatures below 150 °C (Kopf et al. 2002). especially the mobilization of some large ion lithophile elements (LILEs) or high field strength elements (HFSEs), as is shown in Table 3, is surprising giving the collisional setting in the Caucasus. This observation attests that these elements may be released from teh sedimentary phase at PT conditions much lower than the deep subduction factory.

A comparison of our data with those from another set of hydrothermal experiments on a similar mud from the Nankai accretionary prism (You et al. 1996b) is of interest. From the experiments it appears that the strongest increase in fluid B contents occurs above 175 °C. Even at the highest experimental temperature of 350 °C, B devolatilization has apparently not come to a halt (You et al. 1996b). Such temperatures reflect, based on the thermal gradient of ~40°/km in the Caucasus (Kotov and Matienkov 1967), a fluid source depth of about 8–9 km. This value agrees well with depth estimates (Table 4, right column) using other geochemical

proxies for some of the mud domes studied (i.e., 6.7 – 9.3 km for Kuchugurski, Golubicriy, Polivadina, Semigorski, Gladkovskii, Karabetovski, and Shugo MVs; for details see Lavrushin et al. 1996). It also matches the estimated depth of the parent layer, the Maikop mudstones, as inferred from quality seismic data (Cooper 2001). We shall return to this topic when discussing the mobilization and extrusion mechanism (see below).

Mud

Results from both the Taman and Georgia muds show strong B enrichment up to 868 ppm being about 8x higher than clay-rich marine sediments (Ishikawa and Nakamura 1993). The mean B content is 243 ppm for Georgia and 400 ppm for Taman muds, which is in agreement with data on Azerbaijan mud breccias further southwest, where an average 465 ppm was observed (Babayev and Martyrosyan 1973). The high B contents are probably related to the deep burial of some of the mudstones of the parent layers, the Maikop Formation. With burial and time, temperature-driven transformation from smectite to illite has occurred, which is generally accompanied by B uptake into the mineral lattice. Earlier work has shown that illite can incorporate twice as much B into the mineral lattice than smectite (Perry 1970), which apart from the enrichment aspect, also has profound effects on the isotope ratio of the muds.

In order to test whether the mud and fluid are in equilibrium, the B fractionation coefficient α (sometimes termed separation factor s; and defined as $\alpha=(^{10}B/^{11}B)_{mud}\times(^{11}B/^{10}B)_{fluid}$; see Kakihana et al. 1977) can be used. As fractionation of B is strongly influenced by changes in temperature, and consequently in pH, the spectrum of $\delta^{11}B$ values of a mud being in equilibrium with a given fluid can be easily calculated. For the Georgian samples, the average $\delta^{11}B$ fluid signature is 34.2‰ (see Table 4). A corresponding mud in equilibrium with such a fluid would range from +21‰ (at T=20 °C) to +9‰ (at T=400 °C) when based on the experimental boron separation results by Kakihana et al. (1977). The fact that the average Georgian mud is 2.8‰, and even the highest sample (Bayda mud volcano with $\delta^{11}B$=7.4‰; Table 4), well below the calculated value at 400 °C suggests that the muds and fluids may not have been fully equilibrated. We have two possible explanations to offer as an explanation of our observation: First, fluid from another source may explain the mismatch based on B isotope data and may also explain why both muds and fluids are strongly enriched in boron (see below). Second, if a well equilibrated ascended from the Maikop shales to the intermediate depth reservoir observed by Cooper 2001 (see sketch in Fig. 8), the residence time at this shallower level (2–4 km depth) may have altered the B signatures. At present, we feel either explanation, or even a mixture of the two processes could be true.

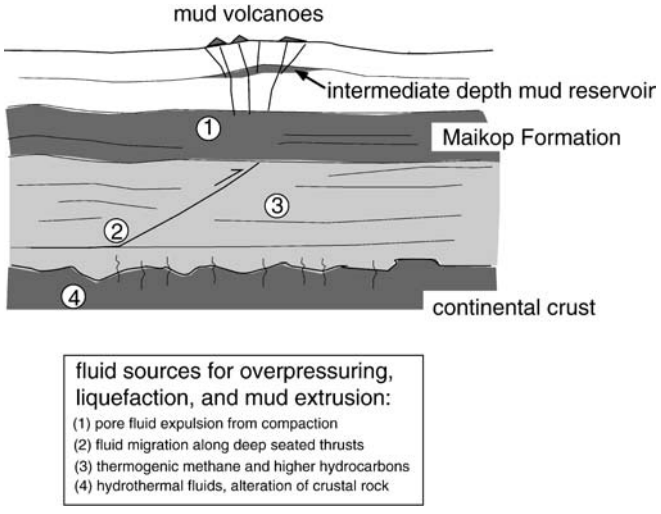

Fig. 8 Schematic diagram of a mud diapir, MV extrusion and diatremes, including possible fluid sources (*numbered 1–4*); mature, B-rich fluids may be found among categories 3, 4, and 7

Previous workers have shown that $\delta^{11}B$ of a sediment decreases with increasing temperature and lithification (Ishikawa and Nakamura 1993; You et al. 1996a). This can be attributed to a number of processes, which quite possibly overlap in vivo. Most of the adsorbed, predominantly "heavy" B isotope is probably lost when the interlayer water of clay minerals is released as a result of tectonic compaction (Fitts and Brown 1999) and transformation of smectite to illite (Colten-Bradley 1987). On the other hand, "light" ^{10}B is preferably incorporated into the mineral lattice, so that with increasing illitization, a more negative $\delta^{11}B$ of the mud would be the consequence (Perry 1970). The majority of our $\delta^{11}B$ results either range in the same order of magnitude as the high T results by You et al. (1996a), or are even more depleted in ^{11}B (e.g., Semigorski, Ahtanizovski, Shugo, Golubicriy, and Gladkovski mud volcanoes). When compared with the boron systematics of ancient and modern marine sediments (Ishikawa and Nakamura 1993), our data coincide in broad terms with the window for modern marine smectite (2.3 – 9.2‰) and continental margin detritus (−13‰ to −8‰), but also with early Miocene slates and claystones from the Shimanto accretionary wedge, southwest Japan (−5.6‰ to −11.7‰). This is in general agreement with results by Chaussidon and Uitterdijk Appel (1997, especially their Fig. 4) who distinguish between two steps of boron fractionation, a first one from seawater to modern clay-rich sediment, followed by a second one to old marine sediment. This latter step is characterized by a drop in $\delta^{11}B$ of about 10‰ (resulting in absolute values around −10‰ for Permian to early Miocene shales; ibid.). A similar observation has been made on sediments in the Nankai Trough where $\delta^{11}B$ values as low as −13‰ are reported from below the décollement at >1 km burial depth (You et al. 1995). Also, metasedimentary rocks from various settings generally have $\delta^{11}B$ results from −6.7‰ to −10.9‰ (Peacock and Hervig 1999). However,

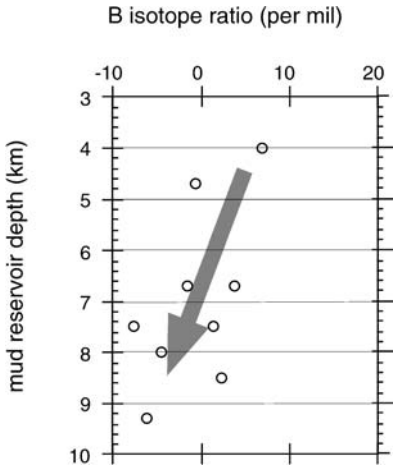

Fig. 9 ^{11}B vs. mud reservoir depth (in km), as estimated for Taman Peninsula mud volcanoes by Lavrushin et al. (1996). Note the distinct depletion of heavy ^{11}B in the mud with depth (as indicated by the *arrow*)

no evidence for metamorphic components has been found in the Caucasian mud breccias. Taken all evidence together, the majority of our results correspond to ancient, marine claystones which have undergone considerable heating (up to 350 °C in case of the Shimanto claystones; Ishikawa and Nakamura 1993). If we tie these observations into the regional geology, the most likely source layer for the mud breccia matrix are mudstones, which were deposited before the marine regression. According to Khain and Malinovski (1963), the transition from a marine to a continental environment with molasse sedimentation occurred during the Miocene and Pliocene. Concerning the regional geology, marine clay-bearing Oligocene/early Miocene rocks of the Maikop Formation are the most likely source rock for the muds. In fact, those deposits have previously been related to Taman MVs and were found in surface outcrops to considerable depth. Since they are believed to partly go back to an origin as olistrostrome deposits, they have been underconsolidated during their entire geological past (Lavrushin et al. 1996). When folded, the Maikop series may reach subsurface depths of 7–10 km (Lavrushin et al. 1996). Such depths are in the same range as estimates based on isotope geochemistry (see Lavrushin et al. 1996; their Table 4). If our B isotope results are plotted versus the depth estimates from these authors, we see a trend of decrease in $\delta^{11}B$ with increasing depth of origin (see Fig. 9).

Mud liquefaction and extrusion

In the second part of the discussion, we want to link the chemical signatures of the muds and waters with the mechanism of mud volcanism. As discussed earlier, B isotope fractionation indicates that mud and pore waters are not fully equilibrated in the Caucasus mud volcanoes. In any case, although they are rapidly deposited, thick argillaceous units of low permeability, it seems unlikely that they preserved enough initial fluid to trigger mud volcanism. Consequently, it has to be concluded that a mature fluid at depth liquefied an already compacted mudstone of the Maikop Formation prior to extrusion. These rocks are buried 4–10 km depending on structural style, and are well mirrored in recent 3D seismic data (Cooper 2001). Fluids from a lateral or deeper source can generate secondary overpressure in low porosity rocks (Moore and Vrolijk 1992), and this may disaggregate the mudstone fabric. Although physical compaction of fine-grained sediments is largely irrecoverable, swelling clays such as smectites or illite may re-adsorb considerable amounts of water, thereby decreasing bulk density of the mud. Being less dense than the overburden, the swelled muds start to ascend along zones of weakness (Fig. 8), forming piercements in fold hinges or exploiting faults or fractures. Initially small quantities of free gas may facilitate this process, since the volume expansion on ascent from depth is enormous (see Brown 1990).

During swelling of the clays, two distinct mechanisms may cause enrichment in certain elements, as will be exemplified using boron. In a first, relatively rapid process, adsorption of dissolved $B(OH)_4^-$ anion occurs at the "frayed-edge" of the clay mineral surface (Couch and Grim 1968). This process may be followed by the much slower diffusion of dissolved B into the clay mineral structure, namely the sheets of linked (Si, Al)O_4 tetrahedra (ibid.). According to the tectonic stress and/or temperature, the distance between these sheets may vary drastically (e.g., Fitts and Brown 1999), so that the efficiency of diffusion and B enrichment is variable (as reflected in the wide range of B contents, e.g., ~143–868 ppm in Taman muds; Table 4). In addition to the diffusion into the lattice, phase transformation of smectite to illite with increasing temperature may also cause considerable secondary B enrichment (Perry 1970).

As a consequence of the numerous variables in the mud volcano system of our study area, our data do not allow us to model B (or Ba, Li) enrichment as a result of residence time of the mature fluid at the parent layer level, the intermediate depth mud reservoir, etc. Also, the temperature at a given depth, or the fluid composition prior to liquefaction, are not known. However, we propose that interaction between the Maikop claystones and the mature waters at depth may have taken place for a considerable period of time for two reasons. First, none of the hydrothermal "long-term" (30 days at elevated T) experiments with high-molarity (up to 1 M) boric acid (Couch and Grim 1968) yielded B uptake in a similar manner as measured in the Caucasian muds. This is very likely a result of insufficient reaction time between mud and fluid to allow for equilibrium water-rock interaction. In contrast, the Caucasian mud domes plot nicely on a curve of other mud volcanoes when B isotope geochemistry is contrasted with temperature (see Kopf and Deyhle 2002, their Fig. 5). The linear trend with progressive illitization of smectite, as observed by these authors, suggests that the systems regarded have reached quasi-

equilibrium. Second, B contents of both fluids (up to 35× seawater) and muds (up to 8× marine sediments) show profound anomalies. Other mobile elements mirror this fluid-rock interaction (Tables 2, 3, 4). As for the source of such a mature fluid having liquefied Maikop claystones, we propose that deep diagenetic (or even metamorphic) reactions in the metasedimentary to crustal levels are the most likely processes. A fluid source from deeper than the Maikop shales, together with a rapid extrusion mechanism, may explain why mud and fluid are apparently not fully equilibrated. Especially the low $\delta^{11}B$ of the mud is a result of the largely completed illitization and other diagenetic processes at depth. In contrast, the B enrichment of the fluid may be due to devolatilization at depth levels of the Maikop formation (down to >10 km), but can also be a consequence of desorption of B from the clay at intermediate depth (i.e., the reservoir at 2–4 km; Cooper 2001).

In summary, the scenario we envisage is that the mud originating from late Tethyan (Oligo-Miocene) marine deposits underwent rapid burial by molasse deposits of the oversteepened Caucasian orogenic wedge after initiation of continental collision in the late Miocene. High sedimentation rates during the Miocene led to rapid accumulation of thick sedimentary sequences (like the Maikop Formation), so that fluid expulsion of the underlying units (Oligocene or older marine pelitic rocks) was severely hindered. Later, a geochemically mature fluid entrains the succession and disaggregates the Maikop claystones to trigger mud volcanism and ascent after continental collision in the late Miocene. There may have been pre-collisionary mud domes extruded from the olistostrome deposits (see Fig. 2A), however, these hardly have been preserved during the orogenesis. All mud domes studied are post-collisional. According to most recent seismic data, muds rose to reservoirs in 2–4 km sub-bottom depth, before they finally extruded (Cooper 2001). Such a model is supported by our $\delta^{11}B$ data that indicate a marine boron enrichment, not a continental environment with molasse deposition (see $\delta^{11}B$ of fluids close to seawater, and $\delta^{11}B$ of muds similar to marine smectite; Table 4). Clay mineral enrichment in B, but also in Ba, Sr and Li, has probably occurred as a function of long-term interaction between mud (namely illite, and to a lesser extent smectite) and the mature fluid. Apart from readsorption after liquefaction, long-term diffusion of the mobile elements into the tetrahedral clay mineral structure (Couch and Grim 1968) as well as illitization (Perry 1970) are the most plausible explanations for the anomalous enrichment patterns found.

Conclusions

From geochemical analyses of mud volcano products being expelled in the Lesser (Georgia) and Greater Caucasus (Taman Peninsula), we can draw the following conclusions:

- Numerous mud volcanoes with up to several hundreds of meters in diameter show evidence for deep-seated dewatering processes within the Caucasus continental collision zone. B isotope study of the mud allows us to estimate its stratigraphic position in the Oligo-Miocene Maikop Formation. As a function of the complex tectonostratigraphic framework in the area, this age bracket corresponds to mud mobilization depths of approximately 7 to 10 km.
- Increasing boron contents and decreasing B isotope ratios of the mud correlate with incipient burial (i.e. depth of mobilization) and progressive illitization. B contents from Taman (average 400 ppm) are higher than from Georgian features (average 243 ppm), and show a similar enrichment as onshore mud volcanoes in Trinidad or Taiwan. The B enrichment of both fluids (relative to seawater) and muds (relative to marine sediment) suggests secondary liquefaction of claystones.
- Regarding the pore fluids of these muds, low chlorinities, but high concentrations of mobile elements suggest that diagenetic fluids interacted with the mud at depth. Boron concentrations in the fluids are enriched by a factor of 5 to 35 relative to modern seawater. Other elements enriched in the fluids include Ba, K, B, Li, Sr, Cs, Cr, U, Th or Y, some of which have previously been thought to become effectively recycled in the volcanic arc (i.e., are only mobilized during melting).
- Given the abundance of boron (and other mobile elements) in the illite- and smectite-rich mud, a two-step mechanism of enrichment in mobile elements is proposed during liquefaction. After rapid chemical adsorption of dissolved B to the clay mineral surface, slower diffusion into the tetrahedral structure of the swelling clay has occurred. Uptake of fluid during swelling, together with hydrocarbon formation nearby, lowered bulk density and hence triggered mud mobilization and extrusion. The mud ascends to intermediate depth (2–4 km) before erupting from that reservoir.
- Of the gases within the fluid phase, CH_4 and CO_2 are most abundant, the first reaching up to 99%vol in places. Methane is of predominantly thermogenic origin (–33.4 to –48.9‰ $\delta^{13}C$), and is estimated to be generated at 80–120 °C ("light" methane) to approximately 250–300 °C ("heavy" methane), corresponding to depths of 2–3 and 6–8 km respectively. This methane may well trigger mud extrusion, especially at shallow levels (upper 2–4 km below the Earth's surface, where the mud reservoir is located). $\delta^{13}C$ isotope ratios of >10‰ are indicative of some minor input of "ultraheavy" CO_2 from possibly the upper continental crust.
- He isotope ratios of the gas phase collected from the mud volcanoes show that the mud fluids from Georgian domes contain some contribution of mantle-derived helium, whereas in their counterparts from the Taman Peninsula He originates from terrestrial

rocks. This is most likely connected to collision-related, deep-seated faulting in the Georgia area where the indenting Dagestan block is thrust beneath the Caucasus massif.

Acknowledgments The authors are grateful for discussion with H. Lange, R.M. Prasolov and I.L. Kamenskii. We especially thank R. Surberg and A. Bleyer for their support during the analyses. B. Bock, E. Zuleger, as well as three anonymous referees are thanked for their criticism on an early draft of this work. More importantly, the helpful suggestions by reviewers H.-J. Brumsack and A.H.F. Robertson helped us to clarify and better illustrate our results. Financial support for the XRD and ICP-MS of the sediments was provided by the EU TMR "large-scale facilities" programme through the University of Bristol (UK). We are also indebted to funding through research grants #00-05-64014 from the Russian Foundation of Basic Researches (VYuL and BGP), Deutsche ForschungsGemeinschaft Zu 80/2-2 (AD) and BASF AG, Germany (AK).

References

Abich H (1863) Über eine im Caspischen Meere erschienene neue Insel nebst Beiträgen zur Kentniss der Schlammvulkane der Caspischen Region. St. Petersburg. Mémoires Acad. Imp. Scientif. St. Petersburg Ser. 7, T6/5, pp 1–137

Andrews JN (1985) The isotopic composition of radiogenic helium and its use to study groundwater movement in confined aquifers. Chem Geol 49:339–351

Babayev NI, Martyrosyan RA (1973) Boron and rare alkalis in the cone breccias of the mud volcanoes of Azerbaijan. Geokhimiya 9:1411–1416

Bagirov E, Nadirov R, Lerche I (1996) Flaming eruptions and ejections from mud volcanoes in Azerbaijan: Statistical risk assessment from the historical records. Energy Explor Exploit 14:535–583

Brown KM (1990) The nature and hydrogeologic significance of mud diapirs and diatremes for accretionary systems. J Geophys Res 95:8969–8982

Brown KM, Westbrook GK (1988) Mud diapirism and subcretion in the Barbados Ridge accretionary complex: the role of fluids in accretionary processes. Tectonics 7:613–640

Brumsack H-J, Gieskes JM (1983) Interstitial water trace metal chemistry of laminated sediments from the Gulf of California, Mexico. Mar Chem 14:89–106

Cantanzaro EJ, Champion CE, Garner EL, Marinenko G, Sappenfield KM, Shields WR (1970) Standard reference material: Boric acid; Isotopic, and assay standard reference materials. Nat Bur Stand (US), Spec Publ 260-17, pp 1–70

Chaussidon M, Utterdijk Appel PW (1997) Boron isotopic composition of tourmalines from the 3.8-Ga-old Isua supracrustals, West Greenland: implications on the ^{11}B value of early Archean seawater. Chem Geol 136:171–180

Colten-Bradley VA (1987) Role of pressure in smectite dehydration—Effects on geopressure and smectite-to-illite transformation. AAPG Bull 71:1414–1427

Cooper C (2001) Mud volcanoes of Azerbaijan visualized using 3D seismic depth cubes: The importance of overpressured fluid and gas instead of non-existent diapirs. Proc EAGE Conf Subsurface sediment mobilisation, Gent, Belgium, Sept 2001, p 71

Couch EL, Grim RE (1968) Boron fixation by illites. Clays Clay Mineral 16:249–256

Craig H (1957) Isotopic standards for carbon and oxygen and correction factors for mass spectrometric analyses of CO. Geochim Cosmochim Acta 12:133–149

Dercourt J, Zonenshain LP, Ricou LE, Kazmin VG, Le Pichon X, Knipper AL, Grandjaquet C, Sbortshikov IM, Geyssant J, Lepvrier C, Pechersky DH, Boulin J, Sibuet J-C, Savostin LA, Sorokhtin O, Westphal M, Bazhenov ML, Lauer JP, Biju-Duval B (1986) Geological evolution of the Tethys belt from the Atlantic to the Pamirs since the Lias. Tectonophysics 123:241–315

Deyhle A (2001) Improvements of boron isotope analysis by positive thermal ionization mass spectrometry using static multi-collection of $Cs_2BO_2^+$ ions. Int J Mass Spec 206:79–89

Deyhle A, Kopf A (2001) Deep fluids and ancient pore waters at the backstop: Stable isotope systematics (B, C, O) of mud volcano deposits on the Mediterranean Ridge accretionary wedge. Geology 29:1031–1034

Dia AN, Castrec-Rouelle M, Boulègue J, Comeau P (1999) Trinidad mud volcanoes: Where do the expelled fluids come from? Geochim Cosmochim Acta 63:1023–1038

Ernst WG, Calvert SG (1969) An experimental study of the recrystallization of porcellanite and its bearing on the origin of some bedded cherts. Am J Sci 267-A:114–133

Fitts G, Brown KM (1999) Stress induced smectite dehydration ramifications for patterns of freshening fluid expulsion in the N. Barbados accretionary wedge. Earth Planet Sci Lett 172:179–197

Gieskes JM, You CF, Lee T, Yui TF, Chen H-W (1992) Hydro-Geochemistry of mud volcanoes in Taiwan. Acta Geol Taiwanica 30:79–88

Goad ST (1816) Miscellaneous observations on the volcanic eruptions at the islands of Java and Sumbawa, with a particular account of the mud volcano at Grobogan. J Sci Arts 1:245–258

Higgins GE, Saunders JB (1974) Mud volcanoes their nature and origin. Verh Naturf Ges Basel 84:101–152

Ishikawa T, Nakamura E (1993) Boron isotope systematics of marine sediments. Earth Planet Sci Lett 117:567–580

Jakubov AA, Ali-Zade AA, Zeinalov MM (1971) Mud volcanoes of the Azerbaijan SSR (in Russian with 17 pp English summary). Publishing house of the Academy of Sciences of the Azerbaijan SSR, Baku

Jenden PD, Hilton DR, Kaplan IR, Craig H (1993) Abiogenic hydrocarbons and mantle Helium in oil and gas fields. In The future of energy gases, USGS Prof Paper 1570, pp 31–56

Kakihana H, Kotaka M, Satoh S, Nomura M, Okamoto M (1977) Fundamental studies on the Ion-xchange separation of boron isotopes. Bull Chem Soc Jpn 50:158–163

Kastner M, Elderfield H, Martin JB (1991) Fluids in convergent margins: what do we know about their composition, origin, role and diagenesis and importance for oceanic chemical fluxes? Philos Trans R Soc Lond A 335:243–259

Khain VE, Milanovski EE (1963) Structure tectonique du Caucase d'après les données modernes. In: Mém Soc Géol Fr, Volume in honour of Prof. Paul Fellot, T. II:663–703

Kopf A, Robertson AHF, Clennell MB, Flecker R (1998) Mechanism of mud extrusion on the Mediterranean Ridge, Geo Mar Lett 18:97–114

Kopf A, Klaeschen D, Mascle J (2001) Extreme efficiency of mud volcanism in dewatering accretionary prisms. Earth Planet Sci Lett 189:295–313

Kopf AJ (2002) Significance of mud volcanism. Rev Geophysics 40/2, 52 pp 10.1029/2000RG000093

Kopf AJ, Deyhle A (2002) Back to the roots: Source depths of mud volcanoes and diapirs using boron and B isotopes. Chem Geol 192:195–210

Kopf AJ, Castillo PR, Deyhle A (2002) Water-Rock interaction in the upper seismogenic zone in the Nankai trough subduction factory. EOS, Trans AGU (Suppl) 83/47:F1294

Kotov VS, Matvienko VN (1967) Geothermal conditions and thermal water resources of Azov-Kuban oil-gas-bearing basin (in Russian). In: Regional geothermics and thermal water distribution in the USSR. Nauka Publ, Moscow, pp 94–102

Lagunova IA (1976) Origin of boron in of mud volcanoes. Int Geol Rev 18:929–934

Lavrushin VU, Polyak BG, Prasolov RM, Kamenskii IL (1996) Sources of material in mud volcano products (based on isotopic, hydrochemical, and geological data). Lith Miner Resour 31(6):557–578

Limonov AF, Kenyon NH, Ivanov MK, Woodside JM (1995) Deep-sea depositional systems of the Western Mediterranean and mud volcanism on the Mediterranean Ridge. UNESCO Rep in Marine Sciences 67, pp 1–172

Mamyrin BA, Anufriev GS, Kamenskii IL, Tolstikhin IN (1970) Determination of the isotopic composition of helium in the atmosphere (in Russian). Geokhimiya 6:721–730

Mamyrin BA, Tolstikhin IN (1981) Isotopes of helium in nature. Elsevier, Amsterdam

Martin JB, Kastner M, Henry P, Le Pichon X, Lallemant S (1996) Chemical and isotopic evidence for sources of fluids in a mud volcano field seaward of the Barbados accretionary wedge. J Geophys Res 101:20325–20345

Mattauer M (1968) Les traits structuraux essentiels de la chaîne Pyréenne. Rev Géogr Phys Géol Dyn 1:3–12

Moore JC, Vrolijk P (1992) Fluids in accretionary prisms. Rev Geophys 30/2:113–135

Palmer MP, Swihart GH (1996) Boron isotope geochemistry: An overview. In Boron: Mineralogy, petrology, and geochemistry. MSA Rev Mineral 33:709–744

Peacock SM, Hervig RL (1999) Boron isotopic composition of subduction zone metamorphic rocks. Chem Geol 160:281–290

Perry A, Jr. (1970) Diagenesis and the validity of the boron paleosalinity technique. Am J Sci 272:150–160

Philip H, Cisternas A, Gvishiani A, Gorshkov A (1989) The Caucasus: an actual example of the initial stages of continental collision. Tectonophysics 191:1–21

Plank T, Langmuir CH (1998) The chemical composition of subducting sediment and its consequences for the crust and mantle. Chem Geol 145:325–394

Polyak BG, Kononov VI, Tolstikhin IN, Mamyrin VA, Khabarin LV (1976) The helium isotopes in thermal fluids. In: Thermal and chemical problems of thermal waters. IAHS Publ 119:17–33

Polyak BG, Tolstikhin IN, Kamensky IL, Yakovlev LE, Marty B, Cheshko AL (2000) Helium isotopes, tectonics, and heat flow in the Northern Caucasus. Geochim Cosmochim Acta 64:1925–1944

Prasolov EM, Lobkov VA (1977) On the conditions of methane generation and migration (based on carbon isotopic composition) (in Russian). Geokhimiya 11:122–135

Robertson AHF & Scientific Party ODP Leg 160 (1996) Mud volcanism on the Mediterranean Ridge: Initial results of Ocean Drilling Program Leg 160. Geology 24:239–242

Robertson AFH (1998) Mesozoic-Tertiary tectonic evolution of the easternmost Mediterranean area: integration of marine and land evidence. In: Robertson AFH, Emeis K-C, Richter C, Camerlenghi A (eds) 1998. Proc ODP, Sci Results 160, College Station, TX (Ocean Drilling Program), pp 723–782

Spivack AJ (1986) Boron isotope geochemistry. Unpubl. PhD Thesis, Woods Hole Oceanographic Inst, Woods Hole, MA, pp 1–184

Spivack AJ, Palmer MR, Edmond JM (1987) The sedimentary cycle of the boron isotopes. Geochim Cosmochim Acta 51:1939–1949

Tamrazyan GP (1972) Peculiarities in the manifestation of gaseous-mud volcanoes. Nature 240:406–408

Valyaev BM, Grinchenko YI, Erokhin VE, Prokhorov VS, Titkov GA (1985) Isotopic mode of mud volcano gases (in Russian). Litol Polesz Iskop 1:72–87

Vinogradov AP, Galimov EM (1970) Carbon isotopes and the origin of petroleum (in Russian). Geokhimiya 3:275–296

Von Breymann MT, Brumsack H, Emeis KC (1992) Depositional and diagenetic behavior of barium in the Japan Sea. Proc Ocean Drilling Program, Sci Results 127/128, pp 651–665

Whiticar MJ (1999) Carbon and hydrogen isotope systematics of bacterial formation and oxidation of methane. Chem Geol 161:291–319

Yassir NA (1989) Mud volcanoes and the behaviour of overpressured clays and silts. PhD Thesis, London, pp 1–249

You CF, Chan LH, Spivack AJ, Gieskes JM (1995) Lithium, boron, and their isotopes in sediments and pore waters of Ocean Drilling Program Site 808, Nankai Trough: Implications for fluid expulsion in accretionary prisms. Geology 23:37–40

You CF, Castillo PR, Gieskes JM, Chan LH, Spivack AJ (1996a) Trace element behavior in hydrothermal experiments: Implications for fluid processes at shallow depths in subduction zones. Earth Planet Sci Lett 140:41–52

You CF, Spivack AJ, Gieskes JM, Martin JB, Davisson ML (1996b) Boron contents and isotopic compositions in pore waters: A new approach to determine temperature-induced artifacts—geochemical implications. Mar Geol 129:351–361

Zitter TAC, Van Der Gaast SJ, Woodside JM (2001) New information concerning clay mineral provenance in mud volcanoes. Proc. 36th CIESM congress, Monaco, 23–28 September 2001, Rapp Comm Int Mer Médit 36:46–47

Zonenshain LP, Le Pichon X (1986) Deep basins of the Black sea and Caspian Sea as remnants of Mesozoic back-arc basins. Tectonophysics 123:181–211